Neutralization of IL-17 rescues amyloid-β-induced neuroinflammation and memory impairment

Cristiano, Claudia; Volpicelli, Floriana; Lippiello, Pellegrino; Buono, Benedetta; Raucci, Federica; Piccolo, Marialuisa; Iqbal, Asif Jilani; Irace, Carlo; Miniaci, Maria Concetta; Perrone Capano, Carla; Calignano, Antonio; Mascolo, Nicola; Maione, Francesco

DOI:
10.1111/bph.14586

Neutralization of interleukin-17 rescues amyloid-β-induced neuroinflammation and memory impairment

Claudia Cristiano[1], Floriana Volpicelli[2], Pellegrino Lippiello[1], Benedetta Buono[1], Federica Raucci[1], Marialuisa Piccolo[1], Asif Jilani Iqbal[3], Carlo Irace[1], Maria Concetta Miniaci[1], Carla Perrone Capano[1,2], Antonio Calignano[1], Nicola Mascolo[1] and Francesco Maione[1,*].

[1]Department of Pharmacy, School of Medicine and Surgery, University of Naples Federico II, Via Domenico Montesano 49, 80131, Naples, Italy.
[2]Institute of Genetics and Biophysics "Adriano Buzzati Traverso", CNR, 80131, Naples, Italy.

[3]Institute of Cardiovascular Sciences (ICVS), College of Medical and Dental Sciences, University of Birmingham, Birmingham, B15 2TT, UK

* **Author for correspondence:** Francesco Maione, Department of Pharmacy, School of Medicine and Surgery, University of Naples Federico II, Via Domenico Montesano 49, 80131, Naples, Italy. Phone: (+39)081678429. E-mail: francesco.maione@unina.it

Running title: Neutralization of IL-17 and neuroinflammation

Word count: 3476

This article has been accepted for publication and undergone full peer review but has not been through the copyediting, typesetting, pagination and proofreading process which may lead to differences between this version and the Version of Record. Please cite this article as doi: 10.1111/bph.14586

Abbreviations: Ab, antibody; AD, Alzheimer's disease ; CNS, central nervous system; Ctrl, control; GCSF, granulocyte-colony stimulating factor; ICAM-1, intercellular Adhesion Molecule 1; ICV, intracerebroventricular; IL-17, Interleukin-17; IN, intranasal; KC, keratinocyte chemoattractant; MCP-5, monocyte chemotactic protein 5; MPO, myeloperoxidase; RT, room temperature; SDF-1, stromal cell-derived factor 1; Th, T helper; TNF, tumor necrosis factor.

Abstract

Background and Purpose: Alzheimer's disease (AD) is a common neurodegenerative disease characterized by a neuroinflammatory state and to date, there is no cure and its treatment represents a large unmet clinical need. The involvement of T helper 17 cells in the pathogenesis of AD-related neuroinflammation has been reported in several studies, however the role of the main cytokine, IL-17, has not been well addressed. Herein, we investigate the effects of IL-17 neutralizing antibody (IL-17Ab) injected by intracerebroventricular (ICV) or intranasal (IN) routes on amyloid-β-induced neuroinflammation and memory impairment in mice.

Experimental Approach: Amyloid-β $(A\beta)_{1–42}$ was injected into cerebral ventricle of adult CD1 mice. These mice received IL-17Ab via ICV either at 1 hour prior to $A\beta_{1–42}$ injection or IN 5 and 12 days after $A\beta_{1–42}$ injection. After 7- and 14-days of $A\beta_{1-42}$ administration, we evaluated olfactory, spatial and working memory and performed biochemical analyses on whole brain and specific brain areas.

Key Results: Remarkably, ICV pre-treatment with IL-17Ab remarkably reduced $A\beta_{1–42}$-induced neurodegeneration, improved memory function and prevented the increase of pro-inflammatory mediators in a dose dependent manner at 7- and 14-days. Similarly, the double IN administration of IL-17Ab after $A\beta_{1–42}$ injection reduced neurodegeneration, memory decline and the levels of pro-inflammatory mediators and cytokines.

Conclusion and Implications: These findings suggest that IL-17Ab reduces neuroinflammation and behavioral symptoms induced by Aβ. The efficacy of IL-17Ab IN

administration in reducing $A\beta_{1-42}$ neurodegeneration points to a possible future therapeutic approach in patients with AD.

Keywords: Alzheimer, Immunotherapy, Intranasal, IL-17, Neuroinflammation.

Introduction

Alzheimer's disease (AD) is a neurodegenerative disorder and one of the most common forms of dementia worldwide (Liu *et al*., 2017). Pathologically, it is characterized by the deposition of extracellular amyloid-β (Aβ) in the brain causing neuronal death in the neocortex and hippocampus leading to irreversible cognitive impairment and behavioral alterations (Taylor *et al*., 2002).

A large body of experimental evidence supports the view that amyloid plaques are (Taylor et al., 2002) key to driving AD pathogenesis through activation of both innate and adaptative immune pathways (Hardy & Selkoe, 2002). The ensued neuroinflammatory response sustains the production and release of neurotoxic and inflammatory mediators (Schwartz & Deczkowska, 2016; Su *et al*., 2016) through the activation of microglia and astrocytes, causing neuronal cell death (Meda *et al*., 1995; Zuroff *et al*., 2017) and the release of inflammatory neurotransmitters and reactive oxygen species (Tansey *et al*., 2007).

The release of mediators leads to recruitment of additional monocytes and lymphocytes through the blood brain barrier, thus promoting their proliferation, and resulting in further release of inflammatory factors (Das & Basu, 2008). Inflammatory markers have been detected not only in the brain but also in the bodily fluids of AD patients, reflecting a systemic neuropathological change (Bagyinszky *et al*., 2017).

T lymphocytes are particularly involved in the inflammatory response associated with AD. It has been shown that activated T cells can easily cross the blood brain barrier contributing to the ongoing inflammatory repertoire and disease pathogenesis (Togo *et al*., 2002). In this context, several studies reported the importance of T helper (Th) 17 cells and Th17-derived pro-inflammatory cytokines such as IL-17, IL-21, IL-22, IL-23, GM-CSF and IFN-γ in the pathogenesis of AD (Saresella *et al*., 2011) and in other neurological disorders such as

multiple sclerosis and Parkinson's disease (Miossec & Kolls, 2012; Tahmasebinia & Pourgholaminejad, 2017)

Increased levels of Th17 transcription factor RORγt, in addition to IL-17 and IL-22, have been found in the brain of AD animal models (Zhang *et al*., 2013; Zhang *et al*., 2015) and the increase of Th17/IL-17A axis is sustained by Aβ-induced oxidative stress (Solleiro-Villavicencio & Rivas-Arancibia, 2017). Furthermore, Zenaro *et al*. (2015) showed a role for neutrophils in AD-like pathogenesis and cognitive impairment through the release of neutrophil extracellular traps and IL-17 into the brain, suggesting that the inhibition of neutrophil trafficking and related neuro-inflammatory onset may be beneficial in this pathology. Therefore, the increased level of IL-17 and the activation of its signal transduction pathway seem to be involved in neurodegeneration and memory impairment, typical of AD (Diaz *et al*., 2012; Yin *et al*., 2009). Moreover, a growing number of studies suggest the involvement of IL-17 in the negative regulation of adult hippocampal neurogenesis (Liu *et al*., 2014), neuronal differentiation and injury (Wang *et al*., 2009).

Given the well-known contribution of neuroinflammation in AD and the stringent involvement of the pro-inflammatory cytokine IL-17, we decided to examined whether the IL-17 neutralizing antibody via intracerebroventricular (ICV) or intranasal (IN) routes could ameliorate amyloid-β-induced neuroinflammation and memory impairment.

Materials and Methods

Reagents

Recombinant mouse IL-17 (also known as IL-17A) neutralizing antibody (IL-17Ab, monoclonal rat IgG_{2A}, clone 50104), its related isotype control (IgG_{2A}, clone 54447) and proteome profiler mouse cytokine Array Kits (cat. ARY006) were purchased from R&D System (Milan, Italy). $A\beta_{1–42}$ (cat. 1428) and $A\beta_{42\text{-}1}$ (cat. 3391) amyloids peptides were purchased from Tocris (Milan, Italy). For western blot analysis, the primary antibodies mouse monoclonal anti-β Amyloid (MOAB-2) were obtained from Novus Biologicals (Milan, Italy). Mouse monoclonal anti-actin was obtained from Sigma–Aldrich Co. (Milan, Italy). The HRP-conjugated IgG secondary antibodies (anti-mouse) were purchased from Dako (Copenhagen, Denmark). For immunofluorescence analysis, the rabbit polyclonal anti-Glial Fibrillary Acid Protein (GFAP) (cat. Z0334) was obtained from Dako Cytomation

(Copenhagen, Denmark) and rabbit anti-ionized calcium binding adapter molecule (Iba-1) (cat. 019-19741) was purchased from Wako Chemicals (Neuss, Germany). The secondary antibody donkey anti-rabbit IgG Alexa Fluor 488 (cat. A21206) was purchased from Invitrogen (USA). The $A\beta_{1-42}$ and S100B kit were purchased from BioVendor (Rome, Italy). Unless otherwise stated, all the other reagents were from Carlo Erba (Milan, Italy).

Animals

CD-1 male mice (10–14 weeks of age, 25–30 g of weight) were purchased from Charles River (Milan, Italy) and kept in an animal care facility under controlled temperature, humidity and on a 12 h:12 h light:dark cycle, with *ad libitum* access to water and standard laboratory chow diet. All experimental procedures were carried out in compliance with the international and national law and policies (EU Directive 2010/63/EU for animal experiments, ARRIVE guidelines and the Basel declaration including the 3Rs concept) (Kilkenny *et al*., 2010; McGrath & Lilley, 2015) and approved by Italian Ministry of Health. All procedures were carried out to minimize the number of animals used (n=6 per group) and their suffering.

***In vivo* animal model and drugs administration**

Mice were randomly divided into 13 experimental groups, as schematically reported in Table 1, counterbalancing body weight variation across groups. For the *in vivo* model, we used a well-established method consisting of a direct Aβ injection as recently described (Maione *et al*., 2018a). Briefly, before the injection, $A\beta_{1-42}$ protein was dissolved in PBS (1μg μl^{-1}) in tubes that were sealed and incubated for 1 day at 37 °C to allow peptide assembly state. Anesthetized mice (mixture of N_2O and O_2 70:30 w v^{-1} containing 2% isoflurane) were injected with aggregated $A\beta_{1-42}$ peptide (3μg $3\mu l^{-1}$) or its inactive control peptide $A\beta_{42-1}$ (3μg $3\mu l^{-1}$) into cerebral ventricle at a rate of 1μl min^{-1}, using a micro-syringe (10μl, Hamilton) according to the procedure previously described (Maione *et al*., 2018a). The needle was removed after 3 min using three intermediate steps with 1-min inter-step delay to minimize backflow. Another experimental group (Ctrl) included mice that received the surgery procedure and Aβ peptide vehicle injection. After surgery and Abs administration, mice were placed on a thermal pad until they awakened. All procedures were performed with strict aseptic manipulation. Hamilton syringe used for ICV injections was repeatedly washed with distilled water followed by flushing with 1 mg ml^{-1} bovine serum albumin solution, in order to avoid non-specific binding of peptides to glass. To evaluate IL-17Ab protection profile

against $A\beta_{1–42}$ peptide-induced amyloidosis, we used two routes of injection: a single ICV administration of IL-17Ab (0.01-1µg $3\mu l^{-1}$) and its related isotype control IgG_{2A} administered at a maximum dose (1µg $3\mu l^{-1}$), 1h prior to the $A\beta_{1–42}$ injection, or IN administration of IL-17Ab (0.01-1µg $10\mu l^{-1}$) and its related isotype control IgG_{2A} administered at highest dose (1µg $10\mu l^{-1}$), at 5 and 12 days post peptide injection (Fig 1). Taking into account several previously published reports (Southam *et al*., 2002; Pires *et al*., 2009), we performed IL-17Ab IN administration considering the effects of volume, body position and anesthesia.

Behavioral studies

At 7- and 14-days post $A\beta_{1-42}$ administration, mice were tested for novel object recognition, olfactory discrimination, Y-maze and Morris water maze (Fig 1). All tests were performed between 9 am and 2 pm in an experimental room with sound isolation and dim light. The animals were carried to the test room for at least 1 hour for acclimation. Behavior was monitored using a video camera positioned above the apparatus and the videos analyzed in a blinded fashion using video tracking software (Any-maze, Stoelting, Wood Dale, IL, USA).

Novel object recognition (NOR)

The NOR task exploits a mouse's natural tendency to explore a novel object after previous exposure to two identical objects. Mice were habituated for 10 minutes into the arena to reduce anxiety associated with the novel arena (plastic arena 30 x 30 x 50 cm). After this habituation stage, mice were ready to perform the task, which was conducted using two trials (familiarization trial [T1] and a test trial [T2]) separated by 30 minutes. During T1, mice were allowed to explore for 10 minutes two identical objects (plastic screw-top tubes) secured to the floor using a small amount of Blu Tack in habituated arenas. For T2, one identical object from T1 was replaced with a novel object (small green flask) and mice were allowed to freely explore for 5 minutes. T1 and T2 were recorded using a video camera and analyzed for the time spent interacting with the novel object. All arenas were cleaned with 80% ethanol prior the test. Novel object exploration was calculated in T2 by (T novel x 100)/(T novel + T identical) with exploration defined as the nose being less than 1 cm from the object when facing the object or actively engaging with the object by sniffing or paw touching. Climbing on the object was not considered exploratory.

Y-maze task

Spontaneous alternation is a measure of spatial working memory. Such short-term working memory was assessed by recording spontaneous alternation behavior during a single session in the Y-maze (made with three arms, 40 cm long, 120°C separate) positioned at the exact same location for all procedures. Each mouse was placed at the end of one arm and allowed to move freely through the maze during a 5 min session. The series of arm entries were visually recorded. An arm choice was considered only when both fore paws and hind paws fully entered into the arm. The Y-maze was cleaned after each test with 80% ethanol to minimize odor cues. Alternation was defined as a successive entrance onto the three different arms. The number of correct entrance sequences (e.g., ABC, BCA) was defined as the number of actual alternations. The number of total possible alternations was therefore the total number of arm entries minus two, and the percentage of alternation was calculated as actual alternations/total alternations x 100 (D'Agostino *et al*., 2012).

Morris water maze

To assess spatial memory function, mice were tested by Morris water maze which consisted of a circular pool (diameter 170 cm, height 60 cm) with a transparent platform (10 cm in diameter), submerged under the water surface (1.5 cm). The water temperature of 24±1 °C, light intensity and external visual cues in the room were rigorously reproduced. Swimming was recorded using a camera capture and analyzed using video tracking software (Any-maze, Stoelting, Wood Dale, IL, USA) that divided the pool into four equal quadrants. The platform position remained stable during 4 days in one of the four quadrants. Training phase consisted of four swims per day for 4 days, with about a 15-min inter-trial time. Each of the four starting positions was used in randomized order. Each trial was started by placing a mouse into the pool, facing the wall of the tank and terminated as soon as the animal reach the platform with a cut-off of 60 s. After the test, each mouse was kept warm for an hour and then returned to their home cage. Average of the four trials for each mouse and then the average for each group to give a single path length and escape latency expressed as mean ± SEM, was calculated for each training day. A probe test was also performed 1 h after the last swim on day 4. The platform was removed and each animal was allowed a free 60 s swim. The time spent in the quadrant where the platform was previously placed, was determined. A higher percentage of time spent in the platform quadrant is interpreted as a higher level of memory retention. All tests were conducted in the morning.

Olfactory discrimination

The task was based on the fact that mice prefer places with their own odor (familiar compartments) instead of places with unfamiliar odors. In this test, mice had access to 2 adjacent identical chambers separated by an intermediate zone. One chamber contained familiar bedding from its home cage over the last 48 hours (familiar) whereas the other contained fresh bedding (non-familiar). Mice were placed individually into the intermediate zone and allowed to freely explore each chamber for 10 minutes. Rodents are capable of discriminating familiar versus non-familiar chambers since they prefer their odor to no odor at all (D'Agostino *et al*., 2012). The time spent in each chamber was recorded and analyzed. An olfactory discrimination index was generated according to the following formula: T familiar/(T familiar + T non-familiar), where T equal time and/or 0.5 as final value were considered as no preference.

Cytokines and Chemokines protein array

All mice were euthanized and brains immediately removed. Total brain, prefrontal cortex and hippocampus (half of the brain was used for cytokine/chemokine analysis and the half for further dissection and related analysis) were collected into a 2.0 ml tube for an immediate preservation in liquid nitrogen and a successive storage at -80°C. The isolated tissues were homogenized in ice-chilled Tris–HCl buffer (20 mM, pH 7.4) containing 0.32 M sucrose, 1 mM EDTA, 1 mM EGTA, 1 mM PMSF, 1 mM sodium orthovanadate and one protease inhibitor tablet per 50 ml of buffer. Protein concentration was determined by the BioRad protein assay kit (BioRad, Italy). Equal volumes (1.5 ml) of the homogenates were then incubated with the pre-coated proteome profiler array membranes according to the manufacturer's instructions. Dot plots were detected by using the enhanced chemiluminescence (ECL) detection kit and Image Quant 400 GE Healthcare software (GE Healthcare, Italy) and successively quantified using GS 800 imaging densitometer software (Biorad, Italy).

Western blot analysis

Whole brain tissue homogenates (35 μg of protein) were subjected to SDS-PAGE (10% gel) using standard protocols as previously described (Blaine Stine *et al*., 2011; Maione *et al*., 2018a). The proteins were transferred to PVDF membranes in the transfer buffer [25 mM Tris–HCl (pH 7.4) containing 192 mM glycine and 20% v/v methanol] at 400 mA for 2 h. The membranes were saturated by incubation for 2 h with non-fat dry milk (5% wt/v) in PBS supplemented with 0.1% (v/v) Tween 20 (PBS-T) for 2 h at RT and then incubated with

1:1000 dilution of anti-β Amyloid or with 1:2000 dilution of anti-actin (after stripping) overnight at 4°C and then washed 3 times with PBS-T. Blots were incubated with a 1:3000 dilution of horseradish peroxidase-conjugated secondary antibody for 2 h at RT, washed 3 times with PBS-T. Protein bands were detected by using the enhanced chemiluminescence (ECL) detection kit and Image Quant 400 GE Healthcare software (GE Healthcare, Italy). Protein bands were quantified using GS 800 imaging densitometer software (Biorad, Italy) and normalized with respective actin.

ELISA assay

Enzyme-linked immunosorbent assay for $A\beta_{1-42}$ and S100B was carried out on brain homogenates. Briefly, 100 µl of tissue supernatants, diluted standards, quality controls and dilution buffer (blank) were added to a pre-coated plate with monoclonal anti-$A\beta_{1-42}$ or S100B for 2 h. After washing, 100 µl of biotin labeled antibody was added for 1 h. The plate was washed and 100 µl of streptavidin-HRP conjugate was added and the plate was incubated for a further 30 min period in the dark. The addition of 100 µl of the substrate and stop solution represented the last steps before the reading of absorbance (measured at 450 nm) on a microplate reader. Antigen levels in the samples were determined using a standard curve of $A\beta_{1-42}$ or S100B and expressed as $\mu g\ ml^{-1}$.

Immunofluorescence analysis

Immunofluorescence was performed by the free-floating method. Briefly, mice were transcardially perfused with phosphate buffered saline (PBS) pH 7.4 solution followed by 4% paraformaldehyde. Brains were removed from the skull and fixed overnight in the 4% paraformaldehyde solution at 4°C. After being transferred in 30% sucrose solution, brains were cut into 25 µm sections using a cryostat microtome (Leica, Wetzlar, Germany) throughout the hippocampus. Slices were blocked for 1 h in 0.1% bovine serum albumin (BSA) solution and then incubated overnight at 4°C with primary antibody for the microglial cell marker Iba-1 (1:1000) or astrocytes cell marker GFAP (1:1000). The day after, sections were washed and incubated for 1 h with secondary antibody solution (donkey anti-rabbit IgG Alexa Fluor 488; 1:1000). Slices were washed, mounted onto glass slides and cover-slipped with Vectashield mounting medium (Vector Laboratories, Burlingame, CA), and images taken by Leica DM RB microscope using the Leica Application Suite software V.4.1.0 and photographed at 20X magnification. For quantification analysis, from each section containing

the hippocampus (bregma level -1.82mm) activated astrocytes and microglia were counted from chosen equal area and analyzed with Image J software (NIH, Bethesda, MD, USA).

Myeloperoxidase assay

Leukocyte myeloperoxidase (MPO) activity was assessed by measuring the H_2O_2-dependet oxidation of 3,3',5,5'-tetramethylbenzidine (TMB) as previously reported (Maione *et al*., 2009). Tissues (total brain) were homogenized for 35 sec in a solution composed of hexadecyltrimethylammonium bromide (HTAB; 0.5% w v^{-1}) in 50 mM sodium phosphate buffer pH 5.4. After homogenization, samples were centrifuged (4000 g) for 20 min and the supernatant used for the assay. Aliquots of 20 µl were incubated with 160 µl of TMB and 20 µl of H_2O_2 (in 80 mM phosphate buffer, pH 5.4) in 96-well plates. Plates were incubated for 5 min at RT and optical density was read at 620 nm using a plate-reader (Biorad, Italy). Assay were performed in duplicates and normalized for protein content.

Statistical analysis

The results obtained were expressed as the mean ± SEM. Statistical analysis were performed by using one-way ANOVA followed by Bonferroni or Dunnett's post-test when comparing more than two groups. GraphPad Prism 6.0 software (San Diego, CA, USA) was used for analysis. Data were considered statistically significant when a value of $P \leq 0.05$ was achieved. The data and statistical analysis comply with the recommendations on experimental design, analysis (Curtis *et al*., 2015) and data sharing and presentation in preclinical pharmacology (George *et al*., 2017; Alexander *et al*., 2018).

Nomenclature of Targets and Ligands

Key protein targets and ligands in this article are hyperlinked to corresponding entries in http://www.guidetopharmacology.org, the common portal for data from the IUPHAR/BPS Guide to PHARMACOLOGY (Harding *et al.*, 2018), and are permanently archived in the Concise Guide to PHARMACOLOGY 2017/18 (Alexander *et al.*, 2017).

Results

IL-17Ab alleviates the $A\beta_{1-42}$-induced olfactory and object recognition impairment in a dose dependent manner

Consistent with the demonstration that olfactory dysfunction occurs at the early stage of amyloid-β-induced pathology, the administration of $A\beta_{1-42}$ (3μg $3\mu l^{-1}$ ICV) significantly decreased the capability of mice to discriminate new and familiar odors when tested 7- and 14-days later (Fig 2A-B) compared to Ctrl and $A\beta_{42-1}$ groups. Interestingly, administration of different doses of IL-17Ab injected both ICV (0.01-1μg $3\mu l^{-1}$) and IN (0.01-1μg $10\mu l^{-1}$) was shown to attenuate the olfactory dysfunction significantly in a dose and time dependent manner, both at 7- and 14-days following $A\beta_{1-42}$-administration.

The administration of $A\beta_{1-42}$ significantly reduced the delta time in the NOR test at day 7 and more significantly at day 14 (Fig 2C-D). Prior single ICV (0.01-1μg $3\mu l^{-1}$) injection of IL-17Ab significantly attenuated the $A\beta_{1-42}$ related impairment in the NOR task in a dose and time-dependent manner compared to Ctrl and $A\beta_{42-1}$ groups (Fig 2C-D). The injection of IL-17Ab IN, at different doses (0.01-1μg $10\mu l^{-1}$) on day 5, after $A\beta_{1-42}$ induced-impairment had no effect on day 7, while after the second IN administration on day 12, the higher dose was shown to reduce the impairment in the NOR test at day 14. IL-17Ab alone and IL-17Ab isotype control administered via ICV and IN did not alter both olfactory and object recognition impairment (Fig 2).

IL-17Ab ameliorates $A\beta_{1-42}$-induced spatial and working memory decline

Based on previous results, we selected the most active doses (1μg for both ICV and IN administration) of IL-17Ab to test spatial and working memory by the Morris water maze and Y-maze test. $A\beta_{1-42}$ (3μg $3\mu l^{-1}$ per mouse, ICV) injection induced an increase of escape latency in Morris water maze, specifically during the second day of the training phase, while the acquisition of the platform position was faster in mice treated with IN injection of IL-17Ab (Fig 3A). All groups showed the same average speed (Fig 3B). Two different cohorts of mice were subjected to the probe test at 7 or 14 day following $A\beta_{1-42}$ injection (Fig 3C-D). The time that $A\beta_{1-42}$ injected mice spent in the target quadrant was significantly shorter on

both day 7 and 14 compared to Ctrl and $A\beta_{42-1}$ groups. On day 7, no significant improvement was observed regarding the time spent in the target quadrant in mice treated with the active doses of IL-17Ab by ICV while the IN route significantly increased the time spent in the target quadrant, compared to mice that received only $A\beta_{1-42}$ (Fig 3C). On day 14, the active doses of IL-17Ab, administered both ICV and IN, significantly increased the time spent in the target quadrant (Fig 3D). No significant effects were observed in IL-17Ab administered ICV or IN alone, $A\beta_{42-1}$ and IL-17Ab isotype control groups (Fig 3). These results were also confirmed by the track plots on day 7 and 14 presented in Fig 3E.

Percent of correct alternations in the Y-maze test was then analyzed on day 7- and 14-days after $A\beta_{1-42}$ injection (Fig 4). Single prior ICV (1μg $3\mu l^{-1}$) administration and double administration of IL-17Ab IN (1μg $10\mu l^{-1}$) after the $A\beta_{1-42}$ significantly attenuated the impairment of spontaneous alternation induced by $A\beta_{1-42}$ on both day 7 and day 14, in equal manner (Fig 4A-C). $A\beta_{1-42}$ and IL-17Ab treatments did not affect the total number of arm entries at these dosages (Fig 4B-D). No significant effects were observed in $A\beta_{42-1}$, IL-17Ab administered ICV or IN alone and in IL-17Ab isotype control groups (Fig 4).

Effect of IL-17Ab administration on $A\beta_{1-42}$, S100B and myeloperoxidase levels

We began our biochemical analysis by confirming the behavioural findings with the association of $A\beta_{1-42}$ level in the brain. As expected, $A\beta_{1-42}$ was significantly higher in the AD group compared to control, while its level was significantly lower in IL-17Ab ICV and IL-17Ab IN treated-group (Fig 5A). This correlation failed to reach significance in $A\beta_{42-1}$, IL-17Ab administered ICV or IN alone and in IL-17Ab isotype control groups. These results were supported by the simultaneously presence of Aβ monomers and large oligomers (most likely dimers and tetramers), at both 7- and 14-days post model induction, in mice injected with fibrillated Aβ peptide compare to not-fibrillated-injected mice (Supplementary Fig 1).

Based on these findings, we decided to examine S100B levels in total brain homogenates by S100B ELISA. As shown in Fig 5B at day 14, $A\beta_{1-42}$ (3μg $3\mu l^{-1}$) induced a significant increase in S100B levels compared to Ctrl and $A\beta_{42-1}$ groups. Single ICV administration of IL-17Ab prior the $A\beta_{1-42}$ (1μg $3\mu l^{-1}$), in addition to repeated administration of IL-17Ab by IN route (1μg $10\mu l^{-1}$), significantly attenuated S100B levels compared to $A\beta_{1-42}$ treated mice. No differences in S100B levels were detected between ICV and IN groups, suggesting that both routes had similar positive effects.

We went onto monitor inflammatory leukocyte infiltration, at day 14 post $A\beta_{1-42}$, by measuring MPO activity in brain homogenates. We found a significant increase in MPO activity in $A\beta_{1-42}$ injected mice compared to Ctrl and $A\beta_{42-1}$ groups respectively. The administration of IL-17Ab by ICV (1μg $3\mu l^{-1}$) did not restore MPO activity that was significantly reduced by IL-17Ab injected IN (1μg $10\mu l^{-1}$) (Fig 5C). No significant effects were observed in IL-17Ab administered ICV or IN alone and in IL-17Ab isotype control groups, in terms of S100B levels and MPO activity (Fig 5B-C).

Effect of IL-17Ab administration on $A\beta_{1-42}$-induced neuroinflammatory activity

Given that $A\beta_{1-42}$ injection induces neuroinflammation we investigated the molecular mechanisms behind the neuroprotective effect of IL-17Ab, by examining both ICV and IN alone (and also their effect prior or after the injection of $A\beta_{1-42}$ induced impairment) on microglial and astrocyte inflammatory responses. To confirm of activation of neural cells, we measured expression of GFAP (a marker of astrocyte activation) and Iba-1 (a marker of microglia cell activation) in the hippocampus for different experimental groups 14 days post $A\beta_{1-42}$ injection. As expected, $A\beta_{1-42}$ injected mice showed a significant increase in the expression of both GFAP and Iba-1 (Fig 6D and Fig 6J) when compared to Ctrl (Fig 6A and Fig 6G). Interestingly, both ICV (1μg $3\mu l^{-1}$) and IN (1μg $10\mu l^{-1}$) injection of IL-17Ab significantly reduced astrocyte and microglial proliferative response and activation compared to mice that received only $A\beta_{1-42}$ (Fig 6E-F and Fig 6K-L). GFAP and Iba-1 staining in animals receiving IL17Ab alone injected ICV or IN was similar to the Ctrl group (Fig 6B-C and Fig 6H-I).

Modulation of pro-inflammatory cyto-chemokines by IL-17Ab

Informed by previous results, we also compared the cytokine and chemokine profiles from total brain homogenates of selected groups which were also used for the histological analysis. A similar analysis was performed on homogenates obtained from the hippocampus and prefrontal cortex. As shown in Fig 7, $A\beta_{1-42}$-treated mice (Fig 7E) displayed a marked increase in pro-inflammatory cytokines and chemokines (reference standards shown in 7A) compared to Ctrl group (Fig 7B). In particular, we observed a significant increase in the expression of classical pro-inflammatory cyto-chemokines such as IL-1α, IL-1β, IL-1r, IL-6, IL-17, MIP-1α/β and TNF-α (Fig 7H-J). In line with our *in vivo* evidence, we observed a

reversion of this pro-inflammatory onset in IL-17Ab ICV-treated mice (Fig 7F) which became more evident after IL-17Ab IN treatment (Fig 7D). In particular, IN treatment induced a significant decrease in terms of IL-1β, IL-17, KC and MIP-2 compared to IL-17Ab ICV treatment (Fig 7H-J).

Interestingly, analyzing the inflammatory profile from homogenized hippocampus (Fig 8A-G) and prefrontal cortex (Fig 8H-N) tissues, we found a different scenario. In the hippocampus, $A\beta_{1-42}$-treated mice presented an increase in ICAM, SDF-1 and, in particular, in IL-17 (Fig 8E) compared to Ctrl (Fig 8B) that were reverted after ICV and IN IL-17Ab administration (Fig 8O). In the prefrontal cortex we observed a striking difference only in terms of IL-17 expression in $A\beta_{1-42}$ group (Fig 8L) that was modulated after IL-17Ab ICV (Figure 8M) and IN (Fig 8N) treated mice. Cyto-chemokines expression in animals receiving IL-17Ab alone injected ICV or IN was similar to Ctrl group in whole brain (Fig 7C-D), hippocampus (Fig 8C-D) and prefrontal cortex (Fig 8J-K).

Discussion and Conclusion

Inflammation comprises a large set of diseases that trigger a wide variety of human disorders. Neurological inflammation and autoimmune disorders are an example of immune-mediated inflammation (Newcombe *et al*., 2018). In local inflammation milieu the concentration of pro-inflammatory cytokines e.g. IL-1, IL-2, IL-6, IL-12, IFN-γ, TNF-α, IL-17 and IL-23 or of the other inflammatory mediators increases (Kempuraj *et al*., 2017). Th1 and Th17 cells are the main cellular mediators responsible for immune-mediated damage that polarize to the site of inflammation in presence of noxious/inflammatory stimuli (D'Acquisto *et al*., 2010).

Many studies have suggested a relationship between inflammation severity and Th17 cell-mediated immune responses (Rostami & Ciric, 2013). The role of Th17 cells has been highlighted in several autoimmune disorders including, MS, Inflammatory Bowel Disease (IBD), Rheumatoid Arthritis (RA) and Systemic Lupus Erythematosus (SLE) as well as in neurological disorders including fronto-temporal dementia, PD, AD and schizophrenia (Liu *et al*., 2014).

AD is the most common and most studied neurodegenerative disorder. It has become a critical issue to human health, especially in aging societies, and therefore it is a research hotspot in the global scientific community (Newcombe *et al*, 2018). It is a multifactorial disorder primarily characterized by amyloid plaques deposition in the brain leading to

irreversible cognitive impairment and neuroinflammation that mainly involves hippocampus and cortex districts (D'Amelio *et al*., 2018). Although Th17 cells have been acknowledged as crucial mediators of AD, the effector cytokine IL-17 responsible for their pathogenicity still remains poorly defined and very little is known on its path-physiological role in CNS regions (hippocampus and prefrontal cortex) normally compromised in this disease.

In this study we demonstrate that the neutralization of IL-17 cytokine results in substantial functional recovery of amyloid-β-induced neuroinflammation and memory impairment. Moreover, we report that IL-17Ab administration (both ICV and IN) can reverse reactive gliosis and neuroinflammation as indicated *ex vivo* by the reduction of $A\beta_{1\text{-}42}$, GFAP, Iba-1, S100B and MPO as well as by the inhibition of typical pro-inflammatory cyto-chemokines in total brain, and more specifically hippocampal and prefrontal cortex regions.

In particular, we show that neutralization of IL-17 by a single ICV administration ameliorates amyloid-β-like symptoms (in terms of olfactory dysfunction, spatial and working memory) both after 7- and 14-days, similarly to what observed after a double IL-17Ab IN administration at day 5 and 12. The difference in terms of time of administration is justified by previous published observations that found a significant increase of Th17 cytokines following 7 days from amyloid-β injection (Zhang *et al*., 2013; Zhang *et al*., 2015). Moreover, very robust effects were observed when the antibody was administered at dose of $1\mu g\ \mu l^{-1}$ compared to the isotype control or antibody itself, consistent with previous *in vivo* reports (Mi *et al*., 2011; Fisher *et al*., 2015; Szabo *et al*., 2017). It is known that a major, yet unmet, objective of neuroprotective/anti-neurodegenerative treatments is to arrest or to slow down the fast progression of cognitive impairments. Contingently, behavioral experiments showed that the Aβ-dependent impairment in terms of spatial learning, reference memory and olfactory memory was dose-dependently prevented and reverted by IL-17Ab treatments.

Due to the particular anatomical features of the nasal cavity, IN administration has been explored as a means of preferential drug delivery to the brain, even though a fraction of the drug may be absorbed by the systemic circulation (Fortuna *et al*., 2014). The route of administration used in our work (IN) ensures high brain concentration levels of IL-17Ab reaching the olfactory bulb and strongly suggests that the antibody was directly transferred to the brain via the olfactory neuronal pathway, circumventing the blood brain barrier. To this aim and accordingly to rigorous published papers (Southam *et al*., 2002; Pires *et al*., 2009),

we have also performed our administration considering the effects of volume, time, body position and anesthesia.

Next, we began our biochemical investigation by confirming the well-replicated behavioural findings with the association of $A\beta_{1-42}$ level in whole brain, as pathology index. As expected, $A\beta_{1-42}$ was significantly higher in the AD group compared with the control group, while its level was significantly lower in IL-17Ab ICV and IL-17Ab IN treated-group. In addition, our biochemical investigation also revealed that IL-17Abs (both ICV and IN) significantly attenuated the production of S100B, a glial-derived protein that is secreted from astrocytes. At low concentrations it is considered a neurotrophic factor and neuronal survival protein during the development of the nervous system (Van Eldik & Wainwright, 2003). Conversely, when overproduced by activated glia, it becomes pathological and influences disease progression by acting as pro-inflammatory cytokine, contributing to the exacerbation of neuroinflammation and neuronal dysfunction. In fact, there is compelling clinical evidence that implicate S100B as a component of the neuroinflammatory cycle that drives AD pathogenesis (Mrak & Griffin, 2005). In this context, it is relevant to highlight that S100B levels are increased in activated astrocytes in the brain regions most severely affected by AD, and its levels correlate with neuritic plaque progression. Additionally, S100B production can be stimulated by mediators associated with AD, including β-amyloid and pro-inflammatory cytokines (Van Eldik & Wainwright, 2003). Collectively, this highlights the crucial role of S100B in AD onset and progression and the relevant effects of IL-17Abs in reducing its expression in mouse whole brain. At confirmation of the amelioration of the inflammatory scenario by IL-17 neutralizing antibodies, we also observed, by the aim of immunofluorescence techniques, that GFAP and Iba-1 expression (as index of astrocytes and microglia activation, Gu *et al*., 2015; Liddelow *et al*., 2017) were markedly reduced after IL-17 Abs treatments.

The vasculature of the blood-brain barrier allows only relatively few leukocytes to enter and survey the healthy central nervous system (CNS) (Lefkowitz & Lefkowitz, 2008). However, during pathological CNS inflammation (including AD), the number of leukocytes adhering to and penetrating the CNS vasculature increases (Crawford *et al*., 2001; Russo *et al*., 2018). Considering that the enzyme myeloperoxidase (MPO) is a heme-protein abundant in circulating phagocytes, tissue neutrophils, and some populations of tissue macrophages but also highly expressed in AD brain, where it co-localized with amyloid plaques (Reynolds *et al*., 1999), its abnormal expression and modulation could represent another important aspect

to be considered in amyloid-related disorders. Our results show that the expression levels of the oxidant producing enzyme MPO is modulated by IL-17Ab both after ICV and IN administration.

In line with previous studies (Xia & Hyman, 1999; Rostasy *et al*., 2003; Walker *et al*., 2017), we also found increased expression of different pro-inflammatory mediators (IL-1α, IL-1β, IL-16, KC, MIP-1, IL-17 and TNF-α) in the total brain of Aβ-treated mice compared to control mice (cytokines and chemokines that are found associated with AD pathological changes). Interestingly, we demonstrate, for the first time, a significant reduction of these pro-inflammatory cascades after both ICV and IN administration of IL-17Ab. Furthermore, the comparison of the inflammatory profile from hippocampus and prefrontal cortex tissues presented a distinctive induction and modulation of ICAM, SDF-1 and IL-17 in $A\beta_{1-42}$-treated group compared to Ctrl with a complete abrogation of IL-17 in both regions after IL-17Ab treatment and a significant reduction of ICAM and SDF-1 only in the hippocampus. This difference could be in part correlated with previous observations that have demonstrated that systemic Th17/IL-17 response appears prior to hippocampal neurodegeneration compare to other CNS districts (Solleiro-Villavicencio & Rivas-Arancibia, 2017).

Endothelial intercellular adhesion molecule-1 (ICAM) does not only mediate firm adhesion of leukocytes to vascular beds but also triggers signalling cascades within the endothelial cell, which play a crucial role in modulating subsequent leukocytes diapedesis in CNS, especially during inflammatory conditions (Adamson *et al*., 1999). Furthermore, a number of recent reports document that drugs interfering with endothelial ICAM-1 signalling, efficiently reduce leukocyte migration both *in vitro* and in animal models of CNS inflammation (Turowski *et al*., 2005). In this scenario, SDF-1 (also known as chemokine CXCL12) could also play a crucial role. While SDF-1 is constitutively expressed in the CNS, its role during neuroinflammation still remains unclear. Several reports have shown that SDF-1 moderates remyelination and synaptic plasticity (Merino *et al*., 2015) and, contextually, its pharmacological inhibition (Azizi *et al*., 2014) alleviates the release of inflammatory mediators in both sciatic nerve injury and bone cancer models (Shen *et al*., 2014) as well as N-methyl-d-aspartate receptor (NMDAR)-mediated neurotoxicity (Sanchez *et al*., 2016).

Taken together, it seems that neutralization of IL-17 could substantially restrain release of synergistic cytokines, and thus, expression of inflammatory mediators, which sustain eventual progression of CNS damage. This scenario is in accordance with our previous

studies where we have demonstrated and emphasized the role of IL-17 as a cytokine that sustains rather than induces inflammation. (Maione *et al*., 2009; Maione *et al*., 2018b).

In conclusion, the experimental findings reported here confirm and extend previous evidence showing that IL-17 is a detrimental factor for AD, where this distinctive cytokine (especially for its selective expression in the hippocampus and prefrontal cortex) could represent a key factor for the "self-amplifying" neuroinflammatory onset typical of amyloid-β--related disease. Under this perspective, future studies will focus on IL-17 brain physiopathology as determinant of the developmental neurotoxicity of widely-diffused CNS-related diseases.

Author contribution

Claudia Cristiano, Floriana Volpicelli, Benedetta Buono, Federica Raucci, Pellegrino Lippiello, Marialuisa Piccolo, and Francesco Maione carried out experiments. Claudia Cristiano, Asif Jilani Iqbal, Carlo Irace, Maria Concetta Miniaci, Nicola Mascolo and Francesco Maione performed data analysis and wrote the paper. Carla Perrone Capano and Antonio Calignano helped with revision of the paper. All authors read and approved the final version of the paper before submission.

Acknowledgments

We would like to thank Dr. Antonio Baiano and also Mr. Giovanni Esposito and Mr. Angelo Russo for animal care and technical assistance.

Conflict of interest

The authors declare that there are no conflicts of interest.

Declaration of transparency and scientific rigour

This Declaration acknowledges that this paper adheres to the principles for transparent reporting and scientific rigour of preclinical research recommended by funding agencies, publishers and other organisations engaged with supporting research.

References

Adamson P, Etienne S, Couraud PO, Calder V, Greenwood J (1999). Lymphocyte migration through brain endothelial cell monolayers involves signaling through endothelial ICAM-1 via a rho-dependent pathway. J. Immunol. 162:2964–2973.

Alexander SPH, Roberts RE, Broughton BRS, Sobey CG, George CH, Stanford SC *et al.* (2018). Goals and practicalities of immunoblotting and immunohistochemistry: A guide for submission to the British Journal of Pharmacology. Br J Pharmacol 175:407-411.

Azizi G, Khannazer N, Mirshafiey A (2014). The Potential Role of Chemokines in Alzheimer's Disease Pathogenesis. Am J Alzheimers Dis Other Demen. 29:415-425.

Bagyinszky E, Giau VV, Shim K, Suk K, An SSA, Kim S (2017). Role of inflammatory molecules in the Alzheimer's disease progression and diagnosis. J Neurol Sci 376:242-254.

Blaine Stine W, Jungbauer L, Yu C, Jo LaDu M (2011). Preparing Synthetic Aβ in Different Aggregation States. Methods Mol Biol 670: 13–32.

Crawford FC, Freeman MJ, Schinka JA, Morris MD, Abdullah LI, Richards D *et al.* (2001). Association between Alzheimer's disease and a functional polymorphism in the Myeloperoxidase gene. Exp Neurol 167:456–459.

Curtis MJ, Bond RA, Spina D, Ahluwalia A, Alexander SPA, Giembycz MA *et al.* (2015). Experimental design and analysis and their reporting: new guidance for publication in BJP. Br J Pharmacol 172:3461–3471.

D'Acquisto F, Maione F, Pederzoli-Ribeil M (2010). From IL-15 to IL-33: the never-ending list of new players in inflammation. Is it time to forget the humble aspirin and move ahead? Biochem Pharmacol. 79:525-534.

D'Agostino G, Russo R, Avagliano C, Cristiano C, Meli R, Calignano A (2012). Palmitoylethanolamide protects against the amyloid-β25-35-induced learning and memory

impairment in mice, an experimental model of Alzheimer disease. Neuropsychopharmacology 37:1784-1792.

D'Amelio M, Puglisi-Allegra S, Mercuri N (2018). The role of dopaminergic midbrain in Alzheimer's disease: Translating basic science into clinical practice. Pharmacol Res 130:414-419.

Das S, Basu A (2008). Inflammation: a new candidate in modulating adult neurogenesis. J Neurosci Res 86: 1199- 1208.

Diaz A, Limon D, Chávez R, Zenteno E, Guevara J (2012). Aβ25-35 injection into the temporal cortex induces chronic inflammation that contributes to neurodegeneration and spatial memory impairment in rats. J Alzheimers Dis 30:505-522.

Fischer JA, Hueber AJ, Wilson S, Galm M, Baum W, Kitson C *et al*. (2015). Combined inhibition of tumor necrosis factor α and interleukin-17 as a therapeutic opportunity in rheumatoid arthritis: development and characterization of a novel bispecific antibody. Arthritis Rheumatol 67:51-62.

Fortuna A, Alves G, Serralheiro A, Sousa J, Falcão A (2014). Intranasal delivery of systemic-acting drugs: small-molecules and biomacromolecules. Eur J Pharm Biopharm 88:8-27.

George CH, Stanford SC, Alexander S, Cirino G, Docherty JR, Giembycz MA *et al*. (2017). Updating the guidelines for data transparency in the British Journal of Pharmacology – data sharing and the use of scatter plots instead of bar charts. Br J Pharmacol 174: 2801–2804.

Gu SM, Park MH, Hwang CJ, Song HS, Lee US, Han SB *et al*. (2015). Bee venom ameliorates lipopolysaccharide-induced memory loss by preventing NF-kappaB pathway. J Neuroinflammation 12:124.

Hardy J, Selkoe DJ (2002). The amyloid hypothesis of alzheimer's disease: Progress and problems on the road to therapeutics. Science 297:353-356.

Kempuraj D, Thangavel R, Selvakumar GP, Zaheer S, Ahmed ME, Raikwar SP *et al*. (2017). Brain and Peripheral Atypical Inflammatory Mediators Potentiate Neuroinflammation and Neurodegeneration. Front Cell Neurosci 11:216.

Kilkenny C, Browne W, Cuthill IC, Emerson M, Altman DG (2010). Animal research: Reporting in vivo experiments: The arrive guidelines. Br J Pharmacol 160:1577-1579.

Lefkowitz DL, Lefkowitz SS (2008). Microglia and myeloperoxidase: a deadly partnership in neurodegenerative disease. Free Radic Biol Med 45: 726-731.

Liddelow SA, Guttenplan KA, Clarke LE, Bennett FC, Bohlen CJ, Schirmer L *et al*. (2017). Neurotoxic reactive astrocytes are induced by activated microglia. Nature 2017 541:481-487.

Liu Q, Xin W, He P, Turner D, Yin J, Gan Y *et al*. (2014). Interleukin-17 inhibits adult hippocampal neurogenesis. Sci Rep 4:7554.

Liu Z, Zhang A, Sun H, Han Y, Kong L, Wang X (2017). Two decades of new drug discovery and development for alzheimer's disease. RSC Advances 7:6046-6058.

Maione F, Paschalidis N, Mascolo N, Dufton N, Perretti M, D'Acquisto F (2009). Interleukin 17 sustains rather than induces inflammation. Biochem Pharmacol 77:878-887.

Maione F, Piccolo M, De Vita S, Chini MG, Cristiano C, De Caro C *et al*. (2018a). Down regulation of pro-inflammatory pathways by tanshinone IIA and cryptotanshinone in a non-genetic mouse model of Alzheimer's disease. Pharmacol Res 129:482-490.

Maione F, Iqbal AJ, Raucci F, Beyrau M, Letek M, D'Acquisto F (2018b). Repetitive exposure of IL-17 into the murine air pouch favours the recruitment of inflammatory monocytes and the release of IL-16 and TREM-1 in the inflammatory fluids. Front. Immunol doi: 10.3389/fimmu.2018.02752.

McGrath JC, Lilley E (2015). Implementing guidelines on reporting research using animals (arrive etc.): New requirements for publication in BJP. Br J Pharmacol 172:3189-3193.

Meda L, Cassatella MA, Szendrei GI, Otvos L, Baron P, Villalba M *et al*. (1995). Activation of microglial cells by [beta]-amyloid protein and interferon-[gamma]. Nature 374:647-650.

Merino JJ, Bellver-Landete V, Oset-Gasque MJ, Cubelos B (2015). CXCR4/CXCR7 molecular involvement in neuronal and neural progenitor migration: focus in CNS repair. J Cell Physiol 230: 27-42.

Mi S, Li Z, Yang HZ, Liu H, Wang JP, Ma YG *et al*. (2011). Blocking IL-17A promotes the resolution of pulmonary inflammation and fibrosis via TGF-beta1-dependent and -independent mechanisms. J Immunol 187:3003-3014.

Miossec P, Kolls JK (2012). Targeting IL-17 and TH17 cells in chronic inflammation. Nat Rev Drug Discov 10:763-776.

Mrak RE, Griffin WST (2005). Glia and their cytokines in progression of neurodegeneration. Neurobiology of Aging 26:349-354.

Newcombe EA, Camats-Perna J, Silva ML, Valmas N, Huat TJ, Medeiros R (2018). Inflammation: the link between comorbidities, genetics, and Alzheimer's disease. J Neuroinflammation 1:276.

Pires A, Fortuna A, Alves G, Falcão A (2009). Intranasal drug delivery: how, why and what for? J Pharm Pharm Sci 12:288-311.

Reynolds WF, Rhees J, Maciejewski D, Paladino T, Sieburg H, Maki RA *et al*. (1999). Myeloperoxidase polymorphism is associated with gender specific risk for Alzheimer's disease. Exp Neurol 155: 31–41.

Rostami A, Ciric B (2013). Role of Th17 cells in the pathogenesis of CNS inflammatory demyelination. J Neurol Sci 333:76-87.

Rostasy K, Egles C, Chauhan A, Kneissl M, Bahrani P, Yiannoutsos C *et al*. (2003). SDF-1alpha is expressed in astrocytes and neurons in the AIDS dementia complex: an in vivo and in vitro study. J Neuropathol Exp Neurol 62:617-626

Russo R, Cattaneo F, Lippiello P, Cristiano C, Zurlo F, Castaldo M *et al*. (2018). Motor coordination and synaptic plasticity deficits are associated with increased cerebellar activity of NADPH oxidase, CAMKII, and PKC at preplaque stage in the TgCRND8 mouse model of Alzheimer's disease. Neurobiol Aging 68:123-133.

Sanchez AB, Medders KE, Maung R, Sánchez-Pavón RP, Ojeda-Juárez D, Kaul M (2016). CXCL12 induced neurotoxicity critically depends on NMDA receptor-gated and L-type Ca2+ channels upstream of p38 MAPK. J Neuroinflamm 13:252.

Saresella M, Calabrese E, Marventano I, Piancone F, Gatti A, Alberoni M *et al*. (2011). Increased activity of Th-17 and Th-9 lymphocytes and a skewing of the post-thymic differentiation pathway are seen in Alzheimer's disease. Brain Behav Immun 25:539–547.

Schwartz M, Deczkowska A (2016). Neurological Disease as a Failure of Brain-Immune Crosstalk: The Multiple Faces of Neuroinflammation. Trends Immunol 37:668-679.

Shen W, Hu XM, Liu YN, Han Y, Chen LP, Wang CC *et al*. (2014). CXCL12 in astrocytes contributes to bone cancer pain through CXCR4-mediated neuronal sensitization and glial activation in rat spinal cord. J. Neuroinflamm 11:75.

Solleiro-Villavicencio H, Rivas-Arancibia S (2017). Systemic Th17/IL-17A response appears prior to hippocampal neurodegeneration in rats exposed to low doses of ozone. Neurologia pii: S0213-4853(17)30194-9.

Southam DS, Dolovich M, O'Byrne PM, Inman MD (2002). Distribution of intranasal instillations in mice: effects of volume, time, body position, and anesthesia. Am J Physiol Lung Cell Mol Physiol 282:L833-9.

Su F, Bai F, Zhang Z (2016). Inflammatory Cytokines and Alzheimer's Disease: A Review from the Perspective of Genetic Polymorphisms. Neurosci Bull 32:469-480.

Szabo PA, Goswami A, Mazzuca DM, Kim K, O'Gorman DB, Hess DA *et al*. (2017). Rapid and Rigorous IL-17A Production by a Distinct Subpopulation of Effector Memory T Lymphocytes Constitutes a Novel Mechanism of Toxic Shock Syndrome Immunopathology. J Immunol 198:2805-2818.

Tahmasebinia F, Pourgholaminejad A (2017). The role of Th17 cells in auto-inflammatory neurological disorders. Prog Neuropsychopharmacol Biol Psychiatry 79:408-416.

Tansey MG, McCoy MK, Frank-Cannon TC (2007). Neuroinflammatory mechanisms in Parkinson's disease: potential environmental triggers, pathways, and targets for early therapeutic intervention. Exp Neurol 208: 1-25.

Taylor JP, Hardy J, Fischbeck KH (2002). Toxic proteins in neurodegenerative disease. Science 296:1991-1995.

Togo T, Akiyama H, Iseki E, Kondo H, Ikeda K, Kato M *et al*. (2002). Occurrence of T cells in the brain of Alzheimer's disease and other neurological diseases. J Neuroimmunol 124:83–92.

Turowski P, Adamson P, Greenwood J (2005). Pharmacological targeting of ICAM-1 signaling in brain endothelial cells: potential for treating neuroinflammation. Cell Mol Neurobiol 1:153-170.

Van Eldik LJ, Wainwright MS (2003). The Janus face of glial-derived S100B: beneficial and detrimental functions in the brain. Restor Neurol Neurosci 3-4:97-108.

Walker DG, Lue LF, Tang TM, Adler CH, Caviness JN, Sabbagh MN *et al*. (2017). Changes in CD200 and intercellular adhesion molecule-1 (ICAM-1) levels in brains of Lewy body disorder cases are associated with amounts of Alzheimer's pathology not α-synuclein pathology. Neurobiol Aging 54:175-186.

Wang DD, Zhao YF, Wang GY, Sun B, Kong QF, Zhao K *et al*. (2009). IL-17 potentiates neuronal injury induced by oxygen-glucose deprivation and affects neuronal IL-17 receptor expression. J Neuroimmunol 212:17-25.

Xia MQ1, Hyman BT (1999). Chemokines/chemokine receptors in the central nervous system and Alzheimer's disease. J Neurovirol 5:32-41

Yin Y, Wen S, Li G, Wang D (2009). Hypoxia enhances stimulating effect of amyloid beta peptide (25-35) for interleukin 17 and T helper lymphocyte subtype 17 upregulation in cultured peripheral blood mononuclear cells. Microbiol Immunol 53:281-286.

Zenaro E, Pietronigro E, Della Bianca V, Piacentino G, Marongiu L, Budui S *et al*. (2015). Neutrophils promote Alzheimer's disease-like pathology and cognitive decline via LFA-1 integrin. Nat Med 8:880-886.

Zhang J, Ke KF, Liu Z, Qiu YH, Peng YP (2013). Th17 cell-mediated neuroinflammation is involved in neurodegeneration of aβ1-42-induced Alzheimer's disease model rats. PLoS One 8:e75786.

Zhang Y, Liu M, Sun H, Yin K (2015). Matrine improves cognitive impairment and modulates the balance of Th17/Treg cytokines in a rat model of Aβ1-42-induced Alzheimer's disease. Cent Eur J Immunol 40:411-419.

Zuroff L, Daley D, Black KL, Koronyo-Hamaoui M (2017). Clearance of cerebral Aβ in Alzheimer's disease: reassessing the role of microglia and monocytes. Cell Mol Life Sci 74:2167-2201.

Table 1. Schematic representation of *in vivo* experimental groups and drugs administration.

Exp. Group	**Group name**	**$A\beta_{42-1}$ ICV**	**$A\beta_{1-42}$ ICV**	**IgG_{2A} ICV**	**IgG_{2A} IN**	**IL-17Ab ICV**	**IL-17Ab IN**
I	Ctrl	-	-	-	-	-	-
II	IL-17Ab ICV	-	-	-	-	1μg $3\mu l^{-1}$	-
III	IL-17Ab IN	-	-	-	-	-	1μg $10\mu l^{-1}$
IV	$A\beta_{42-1}$	3μg $3\mu l^{-1}$	-	-	-	-	-
V	$A\beta_{1-42}$	-	3μg $3\mu l^{-1}$	-	-	-	-
VI	$A\beta_{1-42}$+IgG_{2A}	-	3μg $3\mu l^{-1}$	1μg $3\mu l^{-1}$	-	-	-
VII	$A\beta_{1-42}$ +IL-17Ab ICV	-	3μg $3\mu l^{-1}$	-	-	0.01μg $3\mu l^{-1}$	-
VIII	$A\beta_{1-42}$ +IL-17Ab ICV	-	3μg $3\mu l^{-1}$	-	-	0.1μg $3\mu l^{-1}$	-
IX	$A\beta_{1-42}$ +IL-17Ab ICV	-	3μg $3\mu l^{-1}$	-	-	1μg $3\mu l^{-1}$	-
X	$A\beta_{1-42}$ +IgG_{2A}	-	3μg $3\mu l^{-1}$	-	1μg $10\mu l^{-1}$	-	
XI	$A\beta_{1-42}$ +IL-17Ab IN	-	3μg $3\mu l^{-1}$	-	-	-	0.01μg $10\mu l^{-1}$
XII	$A\beta_{1-42}$ +IL-17Ab IN	-	3μg $3\mu l^{-1}$	-	-	-	0.1μg $10\mu l^{-1}$
XIII	$A\beta_{1-42}$ +IL-17Ab IN	-	3μg $3\mu l^{-1}$	-	-	-	1μg $10\mu l^{-1}$

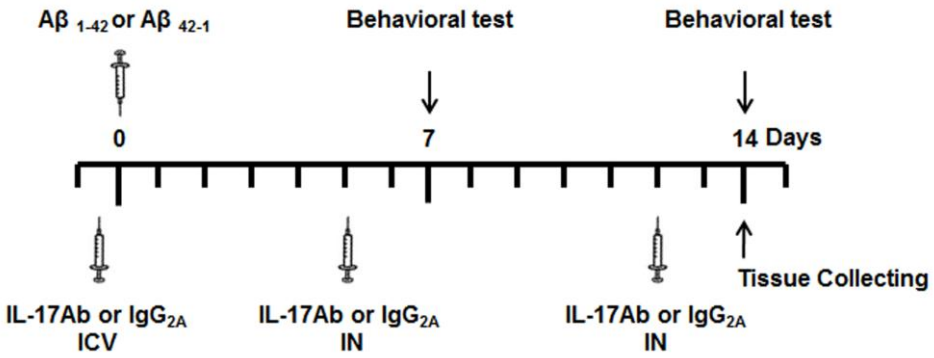

Figure 1. Experimental flow chart for the *in vivo* model, behavioral studies and biochemical and molecular analysis with acute and sub-chronic treatment of IL-17Ab.

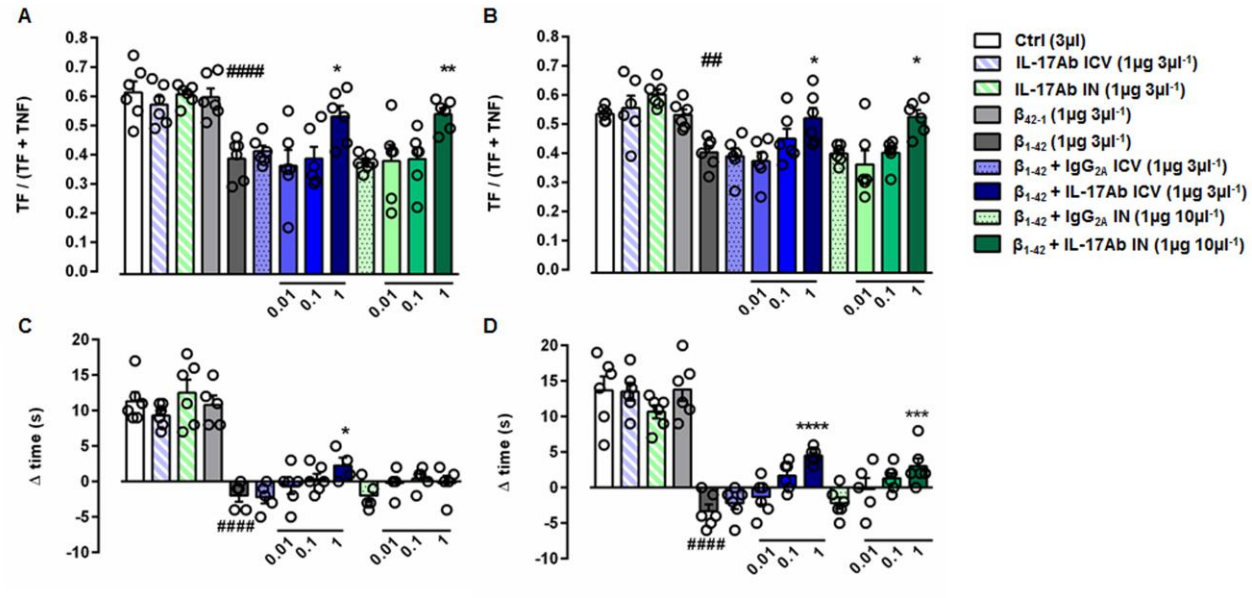

Figure 2. Effect of IL-17Ab ICV and IN-treated mice on (**A-B**) olfactory discrimination at 7-(**A**) and 14-(**B**) days and (**C-D**) on novel object recognition at 7-(**C**) and 14-(**D**) days. Data were expressed as mean ± SEM. Comparisons by one-way ANOVA with Dunnett's post hoc test; $^{\#\#}P \leq 0.01$, $^{\#\#\#\#}P \leq 0.0001$ *vs* Ctrl-treated group; $^{*}P \leq 0.05$, $^{**}P \leq 0.01$, $^{***}P \leq 0.001$, $^{****}P \leq 0.0001$ indicate significance of treatment *vs* $A\beta_{1-42}$ peptide-treated group (N=6 per group).

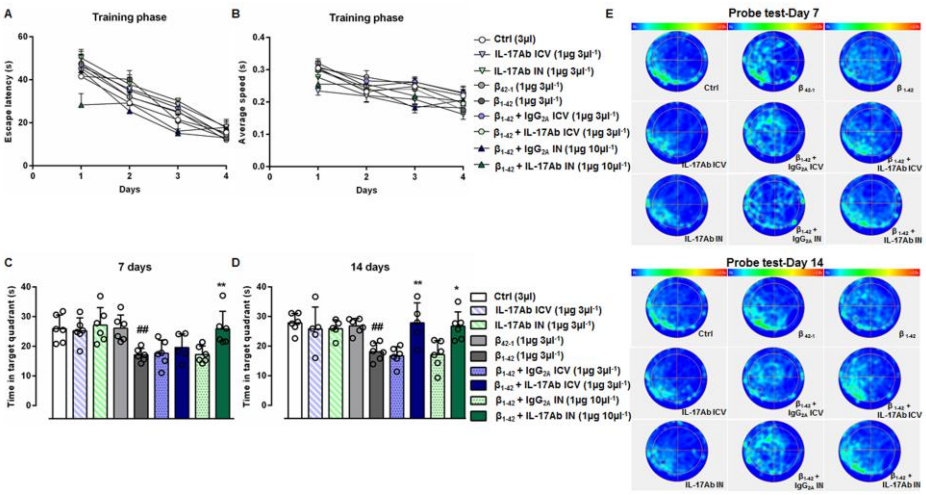

Figure 3. Escape latency (**A**) and average speed (**B**) during training phase in the MWM test. Time spent in the target quadrant of the probe test at 7-(**C**) and 14-(**D**) days. (**E**) Schematic plots of probe test at 7- and 14-days for all experimental groups. Data were expressed as mean ± SEM. Comparisons were by one-way ANOVA with Bonferroni's post hoc test; $^{\#\#}P \leq 0.01$ *vs* Ctrl-treated group; $^{*}P \leq 0.05$, $^{**}P \leq 0.01$ indicate significance of treatment *vs* $A\beta_{1-42}$ peptide-treated group (N=6 per group).

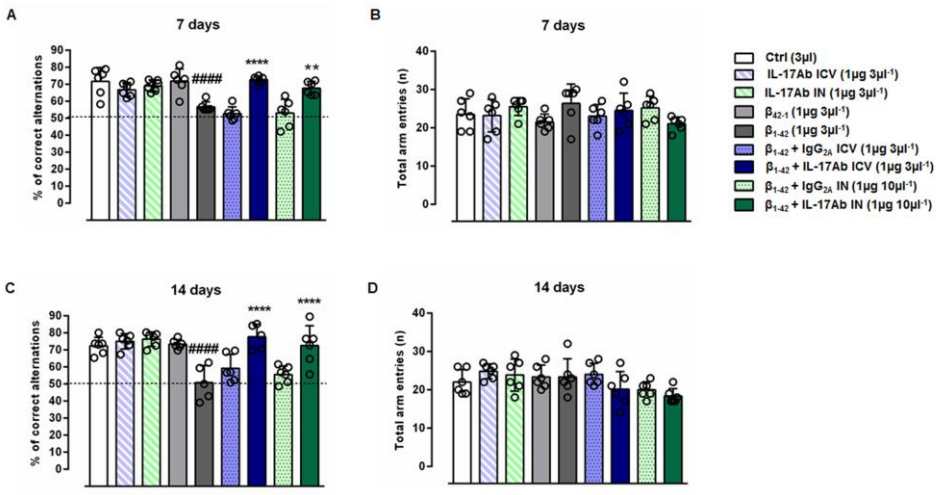

Figure 4. Percent of correct alternations (**A-C**) and total arm entries (**B-D**) in the Y-maze test. Data were expressed as mean ± SEM. Comparisons were by one-way ANOVA with Bonferroni's post hoc test; $^{\#\#\#\#}P \leq 0.0001$ *vs* Ctrl-treated group; $^{**}P \leq 0.01$, $^{****}P \leq 0.0001$ indicate significance of treatment *vs* $A\beta_{1-42}$ peptide-treated group (N=6 per group).

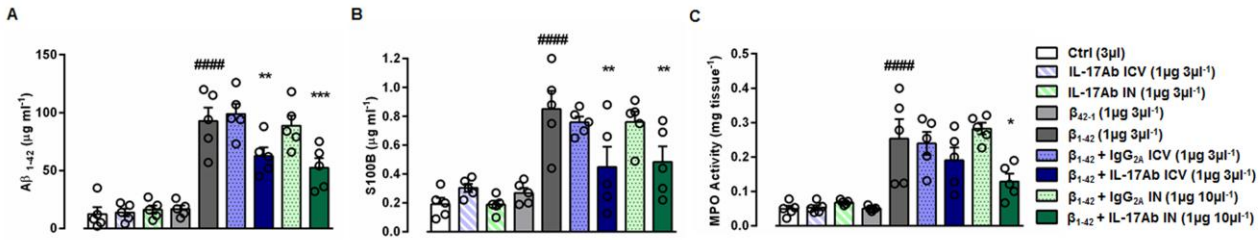

Figure 5. Effect of IL-17Ab on the production of (**A**) $A\beta_{1-42}$ (detected by ELISA assay and expressed as µg ml^{-1}), release of (**B**) S100B protein (detected by ELISA assay and expressed as µg ml^{-1}) and (**C**) MPO activity (detected by enzymatic assay and expressed as mg $tissue^{-1}$) in total brain homogenates. Data were expressed as mean ± SEM. Comparisons were by one-way ANOVA with Dunnett's post hoc test; $^{\#\#\#\#}P\leq0.0001$ *vs* Ctrl-treated group; $^{*}P\leq0.05$, $^{**}P\leq0.01$, $^{***}P\leq0.001$ indicate significance of treatment *vs* $A\beta_{1-42}$ peptide-treated group (N=6 per group).

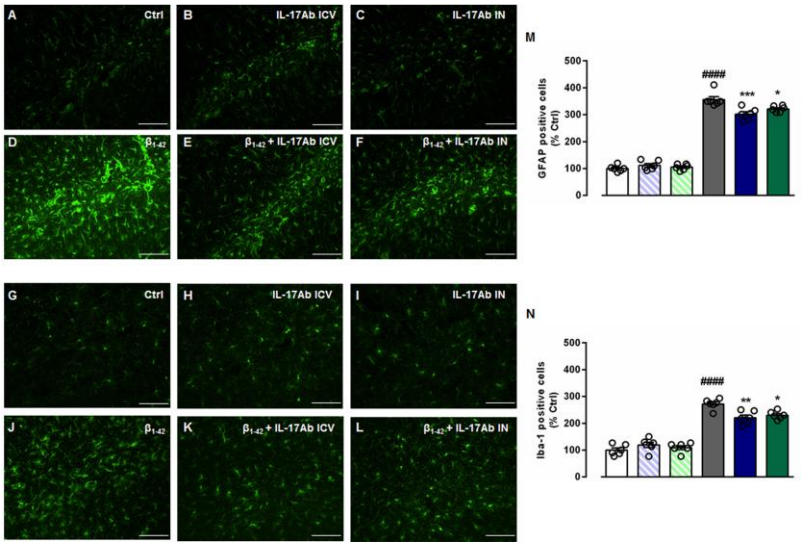

Figure 6. Representative immunofluorescence staining for GFAP and Iba-1 in the hippocampus of (**A-G**) Ctrl, (**B-H**) IL-17Ab ICV, (**C-I**) IL-17Ab IN, (**D-J**) $A\beta_{1-42}$, (**E-K**) $A\beta_{1-42}$ + IL-17Ab ICV or (**F-L**) IL-17Ab IN-treated mice (scale bar 100µm). Quantitative analysis of (**M**) GFAP and (**N**) Iba-1 positive cells. Values are expressed as percent mean (± SEM) of positive cells of n=6 mice in the hippocampus of Ctrl mice. Comparisons were by one-way ANOVA with Bonferroni's post hoc test; $^{\#\#\#\#}P\leq0.001$ *vs* Ctrl-treated group; $^{*}P\leq0.05$, $^{**}P\leq0.01$, $^{***}P\leq0.001$ indicate significance of treatment *vs* $A\beta_{1-42}$ peptide-treated group.

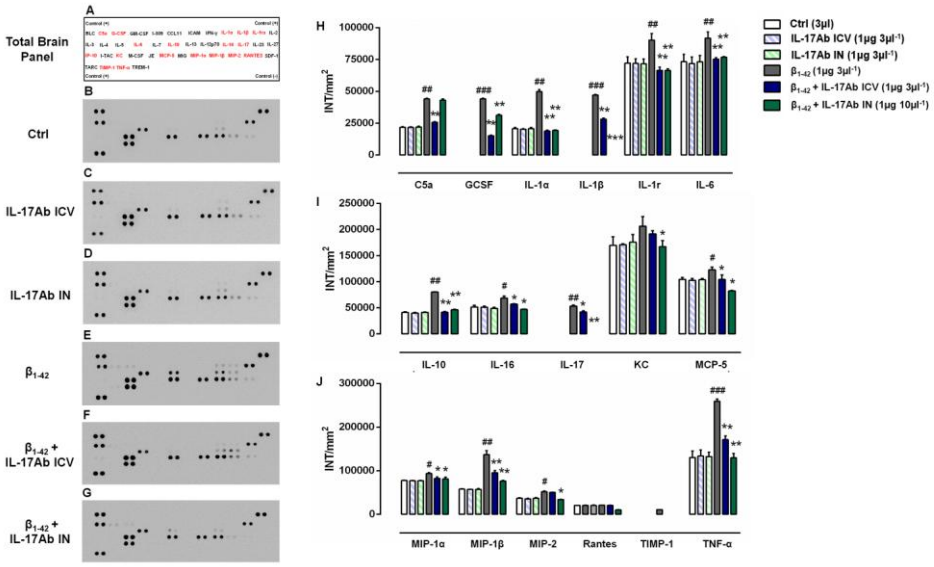

Figure 7. Inflammatory fluids obtained from total brain homogenates of (**B**) Ctrl, (**C**) IL-17Ab ICV, (**D**) IL-17Ab IN, (**E**) $A\beta_{1-42}$, (**F**) $A\beta_{1-42}$ + IL-17Ab ICV or (**G**) IL-17Ab IN-treated mice were assessed using (**A**) a Proteome Profiler cytokine array panel (in red modulated cytokines). Mean changes (± SEM) of positive spots of three separate experiments with n=6 mice, were expressed as INT/mm^2 of densitometric values (**H-J**). Comparisons were by one-way ANOVA with Dunnett's post hoc test; $^{\#}P\leq0.05$, $^{\#\#}P\leq0.01$, $^{\#\#\#}P\leq0.001$ *vs* Ctrl-treated group; $^{*}P\leq0.05$, $^{**}P\leq0.01$, $^{***}P\leq0.001$ indicate significance of treatment *vs* $A\beta_{1-42}$ peptide-treated group.

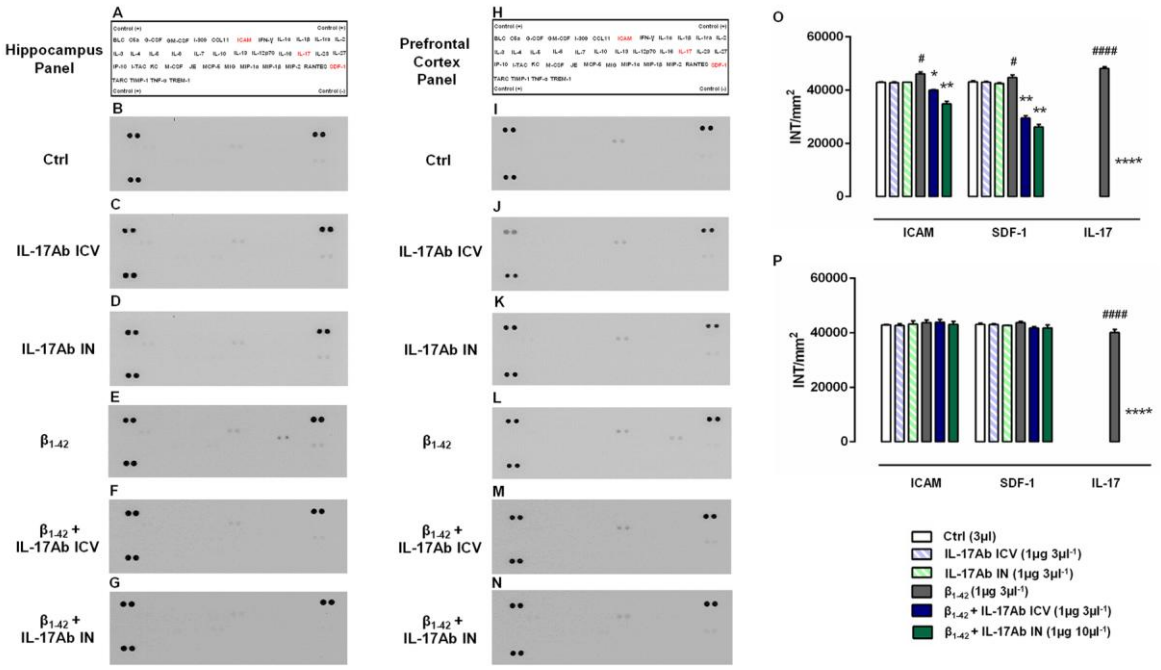

Figure 8. Inflammatory fluids obtained from (**A-G**) hippocampus and (**H-N**) prefrontal cortex homogenates of (**B** and **I**) Ctrl, (**C** and **J**) IL-17Ab ICV, (**D** and **K**) IL-17Ab IN, (**E** and **L**) $A\beta_{1-42}$, (**F** and **M**) $A\beta_{1-42}$ + IL-17Ab ICV or (**G** and **N**) IL-17Ab IN-treated mice were assessed using (**A** and **H**) a Proteome Profiler cytokine array (in red modulated cytokines). Mean changes (± SEM) of positive spots of three separate experiments with n=6 mice, were expressed as INT/mm^2 of densitometric values for both hippocampus (**O**) and prefrontal cortex (**P**). Comparisons were by one-way ANOVA with Dunnett's post hoc test; $^{\#}P\leq0.05$, $^{\#\#\#\#}P\leq0.0001$ *vs* Ctrl-treated group; *P≤0.05, **P≤0.01, ****P≤0.0001 indicate significance of treatment *vs* $A\beta_{1-42}$ peptide-treated group.